

Nonaqueous Sol–Gel Routes to Metal Oxide Nanoparticles

MARKUS NIEDERBERGER*

Department of Materials, ETH Zürich,
Wolfgang-Pauli-Strasse 10, CH-8093 Zürich, Switzerland

Received October 27, 2006

ABSTRACT

Sol–gel routes to metal oxide nanoparticles in organic solvents under exclusion of water have become a versatile alternative to aqueous methods. In comparison to the complex aqueous chemistry, nonaqueous processes offer the possibility of better understanding and controlling the reaction pathways on a molecular level, enabling the synthesis of nanomaterials with high crystallinity and well-defined and uniform particle morphologies. The organic components strongly influence the composition, size, shape, and surface properties of the inorganic product, underlining the demand to understand the role of the organic species at all stages of these processes for the development of a rational synthesis strategy for inorganic nanomaterials.

1. Introduction

Within the broad family of functional materials, metal oxides are particularly attractive with respect to applications in catalysis, sensing, energy storage and conversion, optics, and electronics.¹ For decades they have been extensively investigated by solid-state chemists.² However, to obtain metal oxides as nanoscale materials with well-defined shape, size, and composition, traditional solid-state synthesis based on the reaction of powder precursors is unsuitable. In contrast to these high-temperature processes, soft-chemistry routes, and in particular sol–gel procedures, feature advantages such as the possibility of obtaining metastable materials, achieving superior purity and compositional homogeneity of the products at moderate temperatures with simple laboratory equipment, and influencing the particle morphology during the chemical transformation of the molecular precursor to the final oxidic network.³ Although aqueous sol–gel approaches were highly successful in the synthesis of bulk metal oxides,^{4,5} they brought some major limitations forward when it came to the preparation of their nanoscale counterparts. Aqueous sol–gel chemistry is rather complex, mainly due to the high reactivity of the metal oxide precursors and the double role of water as ligand and solvent. In many cases, the three reaction types (hydrolysis, condensation, and aggregation) occur almost simultaneously (and are difficult to control individually), so

slight changes in experimental conditions result in altered particle morphologies, a serious issue regarding the reproducibility of a synthesis protocol.⁶ Furthermore, the as-synthesized metal oxides are often amorphous, and it is difficult to retain full control over the crystallization process during any additional annealing step. All these parameters might be controlled well enough for the preparation of bulk metal oxides; they, however, represent a big challenge in the case of nanoparticle synthesis.

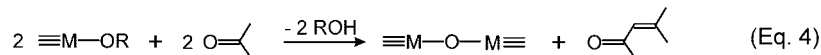
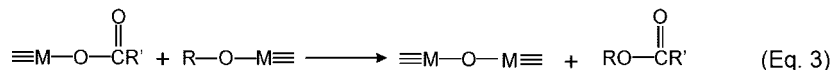
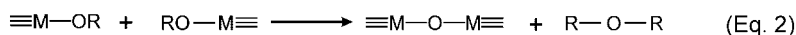
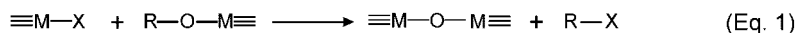
Nonaqueous (or nonhydrolytic) sol–gel processes in organic solvents under exclusion of water are able to overcome some of the major limitations of aqueous systems. The advantages are closely related to the manifold role of the organic components in the reaction mixture. They not only act as the oxygen-supplying agent for the metal oxide but also strongly influence particle size, shape, surface and assembly properties, and, in selected cases, even composition and crystal structure. The slow reaction rates, mainly a consequence of the moderate reactivity of the C–O bond, in combination with the stabilizing effect of the organic species lead to the formation of highly crystalline products that are often characterized by uniform particle morphologies and crystallite sizes in the range of just a few nanometers. Furthermore, nonaqueous sol–gel processes clearly benefit from the fact that the chemistry of the C–O bond is well-established in organic chemistry. This aspect is of utmost significance considering the fundamental role of organic reaction pathways in these synthesis approaches.⁷ Parallel to the formation of the inorganic nanoparticles, also the initial organic species (i.e., solvent and organic constituent of the precursor) undergo transformation reactions that are often based on elementary organic chemistry principles. Identification and quantification of these organic byproducts provide valuable information about the chemical reaction mechanisms leading to the nanoparticles. In contrast to aqueous systems with nearly indefinable composition, the characterization of the organic compounds in organic media can easily be performed with standard techniques like nuclear magnetic resonance (NMR) spectroscopy or gas chromatography–mass spectrometry (GC–MS). By retro-synthetic analysis, it is possible to correlate the processes leading to these organic species to the growth mechanisms of the oxide nanoparticles, offering a powerful tool toward the development of a rational synthesis strategy for a broad family of inorganic nanomaterials.

Although nonaqueous routes to bulk metal oxides never became as popular as aqueous sol–gel approaches, it seems that in nanoparticle synthesis the general trend goes in the other direction, as indicated by the rapidly growing number of papers on nonaqueous sol–gel approaches.^{7,8}

Nonaqueous processes can be divided into two general methodologies, namely, surfactant- and solvent-controlled preparation routes. This Account provides a short over-

Markus Niederberger received his Ph.D. degree from ETH Zürich with Prof. Reinhard Nesper in 2000. After a postdoctoral stay in the group of Prof. Galen D. Stucky at the University of California (Santa Barbara, CA), he joined in 2002 the Colloid Chemistry Department of Prof. Markus Antonietti at the Max Planck Institute of Colloids and Interfaces. In 2007 he became an Assistant Professor in the Department of Materials of ETH Zürich. His primary research interests are the development of general synthesis concepts for inorganic nanoparticles, investigation of formation and crystallization mechanisms, and nanoparticle assembly.

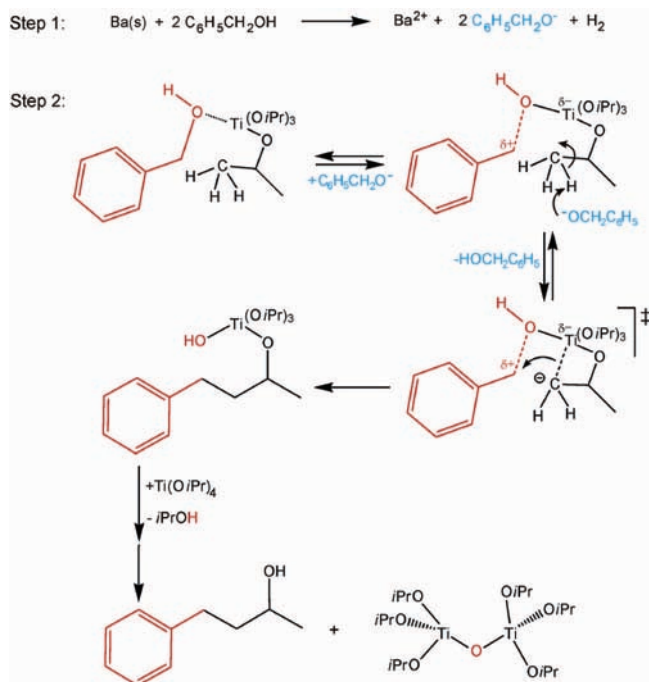
* Corresponding author. E-mail: markus.niederberger@mat.ethz.ch.

Scheme 1. Condensation Steps Leading to M–O–M Bonds in Nonaqueous Sol–Gel Processes [alkyl halide elimination (eq 1), ether elimination (eq 2), ester elimination (eq 3), and aldol-like condensation (eq 4)]

view of these two strategies, highlighting advantages and limitations as well as elaborating some general reaction principles based on selected examples from the literature. It must be pointed out that by definition some of the processes discussed here are not strictly based on sol-gel chemistry. However, as most of them involve the chemical transformation of molecular precursors into the oxidic compound, they are regarded as such in a broader sense.

2. Nonaqueous Sol–Gel Chemistry

The sol-gel process can roughly be defined as the conversion of a precursor solution into an inorganic solid by chemical means. In general, the precursor is either an inorganic metal salt or a metal organic species like a metal alkoxide or acetylacetonate. In aqueous systems, metal alkoxides are the most widely used precursors, and their chemical transformation into the oxidic network involves hydrolysis and condensation reactions.⁵ In aqueous sol-gel processes, the oxygen for the formation of the oxidic compound is supplied by the water molecules. In nonaqueous systems, where intrinsically no water is present, the question of the origin of the oxygen for the metal oxide arises. Analogous to the nonhydrolytic preparation of bulk metal oxide gels,⁹ the oxygen for nanoparticle formation is provided by the solvent (ethers, alcohols, ketones, or aldehydes) or by the organic constituent of the precursor (alkoxides or acetylacetonates). The most frequently found condensation steps in the formation of a metal–oxygen–metal bond are summarized in Scheme 1. Equation 1 displays the condensation between metal halides and metal alkoxides (formed upon the reaction of metal halides with alcohols) under release of an alkyl halide. One of the early examples was the preparation of anatase nanocrystals from titanium isopropoxide and titanium chloride.¹⁰ Ether elimination (eq 2) leads to the formation of a M–O–M bond upon condensation of two metal alkoxides under elimination of an organic ether. This mechanism was reported for the formation of hafnium oxide nanoparticles.¹¹ The ester elimination process involves the reaction between metal carboxylates and metal alkoxides (eq 3), as reported for zinc oxide,¹² titania,¹³ and indium oxide.¹⁴ Analogous to ester eliminations are amide eliminations. Reacting metal oleates with amines, for example, enabled the controlled growth of titania nanorods.¹⁵ In the case of ketones as solvents, the release of oxygen usually involves aldol condensation, where two carbonyl compounds react with each other under (formal)

Scheme 2. Proposed Reaction Mechanism Involving Formation of a C–C Bond for the Simultaneous Generation of BaTiO₃ Nanoparticles and 4-Phenyl-2-butanol (according to ref 7)

elimination of water. The water molecules act as the oxygen-supplying agent for metal oxide formation (eq 4). Literature examples include the synthesis of ZnO¹⁶ and TiO₂^{17,18} in acetone.

However, another more sophisticated pathway has been reported for BaTiO₃, where a C–C coupling mechanism analogous to the Guerbet reaction occurred.¹⁹ In comparison to the “standard” reaction of metal alkoxides in alcohols, which usually proceeds through ether elimination, the only difference from the experimental point of view is the dissolution of metallic barium in benzyl alcohol prior to the addition of the metal alkoxide (step 1 in Scheme 2). Obviously, the presence of benzyl alcoholate induces a different reaction pathway (step 2 in Scheme 2), involving formation of a C–C bond between the isopropoxy ligand of titanium isopropoxide and benzyl alcohol, followed by the formal release of the hydroxyl group from benzyl alcohol. The thus generated Ti–OH group promotes further condensation to the metal oxide under release of 4-phenyl-2-butanol.¹⁹

The synthesis route to BaTiO₃ nanoparticles in benzyl alcohol represents an instructive example for revealing

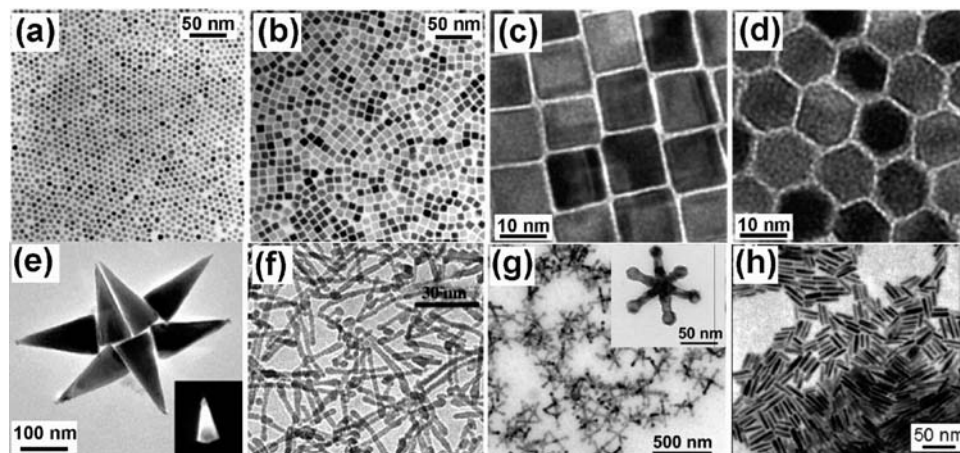


FIGURE 1. TEM images of (a) 8-nm-sized spherical CoFe_2O_4 nanoparticles used as seeds and (b) cubelike CoFe_2O_4 nanoparticles. Reproduced from ref 25. Copyright 2004 American Chemical Society. TEM images of (c) cubelike and (d) polyhedron-shaped MnFe_2O_4 nanoparticles. Reproduced from ref 26. Copyright 2004 American Chemical Society. (e) TEM image of conelike ZnO nanocrystals (inset, dark field TEM image of one crystal). Reproduced from ref 12. Copyright 2005 Wiley-VCH. (f) TEM image of TiO_2 nanorods. Reproduced from ref 13. Copyright 2006 Wiley-VCH. (g) TEM image of MnO multipods (inset, hexapod). Reproduced from ref 27. Copyright 2005 American Chemical Society. (h) TEM image of tungsten oxide nanorods. Reproduced from ref 28. Copyright 2005 American Chemical Society.

and highlighting some basic principles of nonaqueous sol-gel processes. The presence of 4-phenyl-2-butanol as the main species and the near absence of organic ethers in the final reaction solution prove that the formation of the metal oxide does not involve an ether elimination process. The retro-synthetic analysis of 4-phenyl-2-butanol provides a mechanistic model on a molecular level, how the oxygen is formally transferred from the solvent benzyl alcohol to the titanium center, finally building up the metal oxide unit. On the other hand, the high crystallinity of the nanoparticles is most likely a direct consequence of the complex organic reaction pathway, which leads to the slow and controlled release of the hydroxyl group as a condensation agent. Finally, information about the synthesis parameters that direct the reaction along a specific pathway can be obtained. If only $\text{Ti}(\text{O}i\text{Pr})_4$ is reacted with benzyl alcohol under equal experimental conditions, anatase nanoparticles are formed via ether elimination. However, addition of alkaline species such as $\text{Na}(\text{OEt})$ or $\text{K}(\text{OtBu})$ to the reaction mixture results in nanoparticle formation involving the C-C coupling mechanism, clearly underlining that “alkaline” conditions are a prerequisite for the occurrence of this reaction pathway in the Ti system.

3. Nonaqueous Sol-Gel Routes to Metal Oxide Nanoparticles

3.1. Surfactant-Controlled Synthesis of Metal Oxide Nanoparticles. In 1993, Murray et al. published the synthesis of monodisperse CdX ($X = \text{S}, \text{Se}, \text{or Te}$) nanocrystallites in molten trioctylphosphine oxide (TOPO).²⁰ This work provided the basis for the so-called hot-injection method, which involves the injection of a room-temperature solution of precursor molecules into a hot solvent in the presence of surfactants.²¹ The use of surfactants, generally consisting of a coordinating head group and a long alkyl chain, offers several advantages. The coating of the nanoparticles prevents agglomeration

during synthesis and results in good colloidal stability of the final product in organic solvents. Dynamic adsorption and desorption of surfactant molecules onto particle surfaces during particle growth, sometimes combined with selectivity toward specific crystal faces, enables control over particle size, size distribution, and morphology.²² Moreover, the surfactants can be exchanged against other ones in a postsynthetic step, allowing the chemical modification of the surface properties of the nanoparticles.

The technologically important class of magnetic nanoparticles such as iron oxides and ferrites represents a particular track story of surfactant-controlled reaction approaches.²³ The control over particle size has reached such a sophisticated level that it is possible to prepare iron oxide nanoparticles in the size range of 6–13 nm in one nanometer increments.²⁴ In the case of ferrite MFe_2O_4 ($M = \text{Fe}, \text{Co}, \text{or Mn}$) nanoparticles, not only size but also shape control was achieved.^{25,26} The synthesis involved the nonhydrolytic reaction of metal acetylacetonates as precursors with 1,2-hexadecanediol, oleic acid, and oleylamine. The particle size was determined by the amount of precursor; i.e., a higher concentration of acetylacetonates led to larger ferrite nanocrystals. Whereas Song et al. started from spherical CoFe_2O_4 seed particles 8 nm in diameter (Figure 1a) and transformed them into cubelike nanocrystallites with an edge length of 10 nm (Figure 1b) by adjusting the heating rate,²⁵ Zeng et al. systematically varied the surfactant-to-iron acetylacetonate ratio, which resulted in cubelike (Figure 1c) or polyhedron-shaped (Figure 1d) MnFe_2O_4 nanoparticles.

Panels e–h of Figure 1 present TEM images of selected examples of nanoparticles with elongated and branched particle shapes. The thermal treatment of zinc acetate in dioctyl ether, trioctylphosphine oxide, and oleic acid, followed by the addition of 1,12-dodecanediol, resulted in the formation of ZnO nanocrystals with a conelike morphology with an average size of 70 nm (base) ×

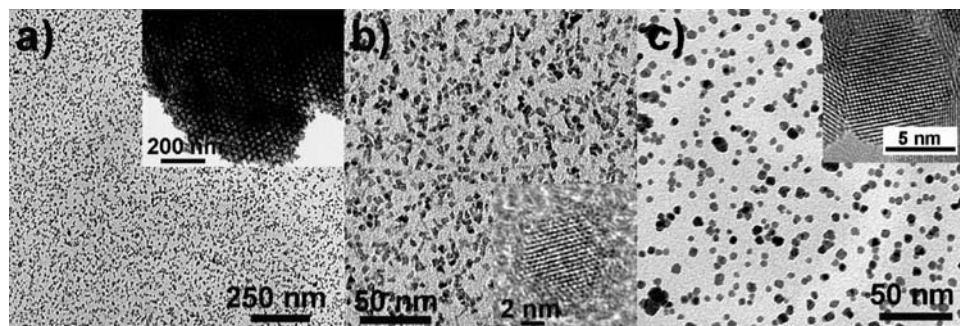


FIGURE 2. (a) TEM image of SnO₂ nanocrystal sol (inset, TEM image of mesoporous SnO₂ after calcination). Reproduced from ref 35. Copyright 2005 Wiley-VCH. (b) TEM image of BaTiO₃ nanocrystals (inset, HRTEM image of one crystal). (c) TEM image of indium tin oxide (10 wt % SnO₂) nanocrystals (inset, HRTEM image of one crystal). Reproduced from ref 42. Copyright 2006 American Chemical Society.

170 nm (height) (Figure 1e).¹² In the case of titania nanorods, the synthesis involved the solvothermal reaction of titanium butoxide, linoleic acid, triethylamine, and cyclohexane.¹³ The titania nanorods exhibit uniform diameters of 3.3 nm, and a length of up to 25 nm, often with a spherical nanoparticle attached to one side of the rod (Figure 1f). MnO multipods were synthesized from a manganese oleate complex in oleic acid and oleylamine (Figure 1g).²⁷ The dissolution of WCl₄ in oleic acid and oleylamine yielded after heat treatment at 350 °C tungsten oxide (W₁₈O₄₉) nanorods, 4.5 nm in width and 28 nm in length (Figure 1h).²⁸

These examples on one hand nicely illustrate the potential of surfactant-controlled synthesis approaches in achieving complex crystal morphologies with outstanding uniformity but, on the other hand, reveal the major limitation of these methodologies. In most of the cases, the synthesis routes are isolated efforts without any generally valid basic concepts or mechanistic principles that would allow a rational synthesis strategy. This statement is supported by a closer look at the chemicals employed in these procedures: five different metal oxide precursors and more than half a dozen of surfactants, often two or three of them in the same reaction batch. However, especially in surfactant-directed synthesis routes with their high content of organic compounds, it is crucial to have a closer look at the organic reaction pathways. In this context, it is not surprising that several research groups started to investigate the organic side reactions also in the synthesis of colloidal group II–VI semiconductor nanocrystals.^{29,30}

3.2. Solvent-Controlled Synthesis of Metal Oxide Nanoparticles. In comparison to the synthesis of metal oxides in the presence of surfactants, the solvent-controlled approaches are considerably simpler. The initial reaction mixture just consists of two components, the metal oxide precursor(s) and a common organic solvent. The small number of reactants simplifies the characterization of the final reaction solution and, related to that, the elucidation of the chemical reaction mechanisms. The synthesis temperature is typically in the range of 50–200 °C, which is notably lower than that in the hot-injection method. But the main advantage of surfactant-free synthesis methods clearly lies in the improvement in product purity. Whereas surface-adsorbed surfactants

influence the toxicity of nanoparticles³¹ and lower the accessibility of the nanoparticle surface in catalytic and sensing applications, these problems are not an issue in nanopowders obtained by surfactant-free routes.

The surfactant-free synthesis methodologies developed in the last few years make use of a large variety of metal oxide precursors such as metal halides, acetates, acetylacetonates, and alkoxides and also include mixtures of different precursors in the case of both compositionally more complex oxides and doping experiments.^{7,32,33} Potential solvents are oxygen-containing organic solvents such as alcohols, ketones, or aldehydes as well as oxygen-free solvents like amines or nitriles with short alkyl chains. Even “inert” solvents such as toluene or mesitylene can be used. The choice of the appropriate solvent mainly depends on its role during nanoparticle growth and also on the targeted morphological as well as compositional characteristics of the final product. Whereas oxygen-containing solvents generally supply the oxygen for the formation of the oxidic compound, nonoxygenated solvents rely on the use of oxygen-containing precursors that are chemically transformed into the metal oxide. The organic solvent and/or the organic species formed during the reaction course act as capping agents, which bind to the particle surface and thus limit the crystal growth and influence particle morphology as well as assembly behavior. Highly stabilizing organic species on the one hand suppress crystal growth and on the other hand can show selectivity toward the binding to different crystal facets, which leads to anisotropic crystal growth. Moreover, the redox properties of the organic solvent can have a strong effect on the chemical composition of the inorganic component.

The simplest nonaqueous and surfactant-free synthesis route to metal oxide nanoparticles involves the reaction of metal halides with alcohols.³⁴ Many metal chlorides readily react with ethanol or benzyl alcohol to the corresponding metal oxides.⁷ In the case of SnO₂, the obtained nanoparticles are well dispersible in tetrahydrofuran without any additional stabilizing agent (Figure 2a), which enables their use as crystalline nanobuilding blocks for the preparation of mesoporous materials by evaporation-induced self-assembly (Figure 2a, inset).³⁵ In general, the reaction between metal halides and alcohols occurs at low reaction temperatures, which makes this synthesis system

particularly useful in cases where organic ligands are required either to functionalize the surface,³⁶ to modify the particle morphology,³⁷ or to control the assembly behavior.^{38,39}

If halide impurities in the final oxidic product are a problem, synthesis routes based on the reaction of metal acetates, acetylacetonates, or alkoxides with alcohols or amines represent a halide-free alternative.⁷ The glycothermal method involving the reaction of metal alkoxides or acetylacetonates in 1,4-butanediol is a versatile approach to various metal oxides.⁴⁰ Another powerful reaction system is based on the use of metal alkoxides and benzyl alcohol, which can be applied to a wide range of binary and multi-metal oxides.^{7,32} As a representative example, a TEM overview image of BaTiO₃ nanocrystals is displayed in Figure 2b, together with a HRTEM image of one particle as an inset.⁴¹ The well-developed lattice fringes prove the high crystallinity. The synthesis of metal oxides containing two or more metals is generally a delicate issue due to the different reactivity of the metal oxide precursors. In contrast to aqueous systems, where this problem is particularly pronounced, the slower reaction rates in organic solvents facilitate the search for metal oxide precursors with the same reactivity toward a specific solvent. The use of chemically different precursors represents an elegant method for the preparation of phase-pure multi-metal oxides with complex composition, as shown for indium tin oxide nanoparticles, where indium acetylacetonate and tin *tert*-butoxide were reacted with benzyl alcohol.⁴² This process enabled the variation of the dopant concentration in a broad range of 2–30 wt %. The nanoparticles exhibit a spherical morphology with diameters of 5–10 nm (Figure 2c) and high crystallinity (Figure 2c, inset). Without additional annealing, these nanopowders exhibited good electrical conductivity.

Alcohols as solvents are not suitable for metal oxides containing cations that are sensitive toward reduction to the respective metals (especially copper- and lead-containing compounds). Ketones and aldehydes represent a nonreductive class of solvents that can be used for such and other oxidic materials like ZnO,¹⁶ BaTiO₃,⁴³ TiO₂,^{17,18} In₂O₃,³³ BaSnO₃,³² PbTiO₃, Pb(Zr,Ti)O₃, and PbZrO₃.⁴⁴

Interestingly, the synthesis of metal oxide nanoparticles can also be performed in oxygen-free solvents provided that the precursor contains oxygen atoms. Zirconium and titanium alkoxides were transformed into the respective oxides by thermal decomposition in inert organic solvents like toluene.^{45,46} Other reaction systems make use of nitrogen-containing solvents. The reaction of metal acetylacetonates with benzylamine yielded nanocrystalline iron, zinc, indium, and gallium oxide,⁴⁷ whereas acetonitrile as a solvent led to indium and zinc oxide.⁴⁸

4. Remarks on the Role of the Organics

The investigation and classification of the chemical reaction mechanisms leading to metal oxide formation in solvent-controlled processes provide a big step forward in the development of a rational synthesis strategy for

inorganic nanoparticles. However, as long as general concepts for the correlation of a particular synthesis system with the final particle morphology are missing, this progress cannot unfold its full potential. The difficulty and complexity of finding answers to this crucial question are shown in this section using selected examples, where seemingly simple reaction mixtures lead to not only spherical nanoparticles but also well-defined organic–inorganic nanostructures.

Yttrium and lanthanide isopropoxides (Ln = Gd, Sm, Nd, or Er) react with benzyl alcohol to form ordered nanohybrids consisting of thin crystalline oxide layers (~0.6 nm) equally separated from each other by an organic layer of intercalated benzoate molecules.^{49,50} A mechanism in which hydride-transfer reactions form benzoic acid and toluene from benzyl alcohol via benzaldehyde, catalyzed by the growing metal oxide species, was proposed. The benzoate molecules obviously restrict the growth of the metal oxide and direct their assembly into the hybrid structure. As a representative example, Figure 3a shows TEM images of the neodymium oxide–benzoate nanohybrid.⁵⁰ However, benzoate molecules formed *in situ* are also able to induce the growth of nanoparticles with a one-dimensional morphology. The reaction of lanthanum isopropoxide in a mixture of benzyl alcohol and 2-butanone in the presence of potassium permanganate yielded La(OH)₃ nanoparticles with a fibrous shape (Figure 3b). The anisotropic particle growth is presumably a direct consequence of the benzoate molecules that bind selectively to specific faces of the lanthanum hydroxide crystal. The reaction of tungsten isopropoxide with benzyl alcohol represents an example in which another oxidation product of benzyl alcohol played the critical role in determining particle shape and assembly behavior.⁵¹ The as-synthesized tungsten oxide consists of nanowire bundles that are held together by intercalated benzaldehyde molecules. The bundles can be split up into individual nanowires with uniform diameters of 1 nm by the addition of formamide to a dispersion of the nanobundles in ethanol (Figure 3c). In spite of the tiny diameter and the high structural flexibility, the nanowires are well crystalline as proven by the selected area electron diffraction (SAED) pattern (Figure 3c, inset).

The sensitivity of the morphological characteristics of the final inorganic product to slight chemical changes in the solvent is nicely illustrated in the case of tungsten oxide nanoplatelets. Whereas the reaction of tungsten chloride with benzyl alcohol yielded tungstite nanoplatelets with a relatively broad size distribution in the range of 30–100 nm (Figure 3d),³⁴ the same process in 4-*tert*-butylbenzal alcohol resulted in the formation of a fibrous network (Figure 3e).⁵² A TEM image at a higher magnification reveals that these ribbonlike structures consist of parallel columns with uniform diameters of 4 nm (Figure 3f). Each nanocolumn is composed of self-aligned nanoplatelets 1 nm thick and facing each other along the entire length of the nanostack. The individual nanostacks are nearly monodisperse in diameter as a consequence of the uniform-sized platelets, which leads to an outstanding

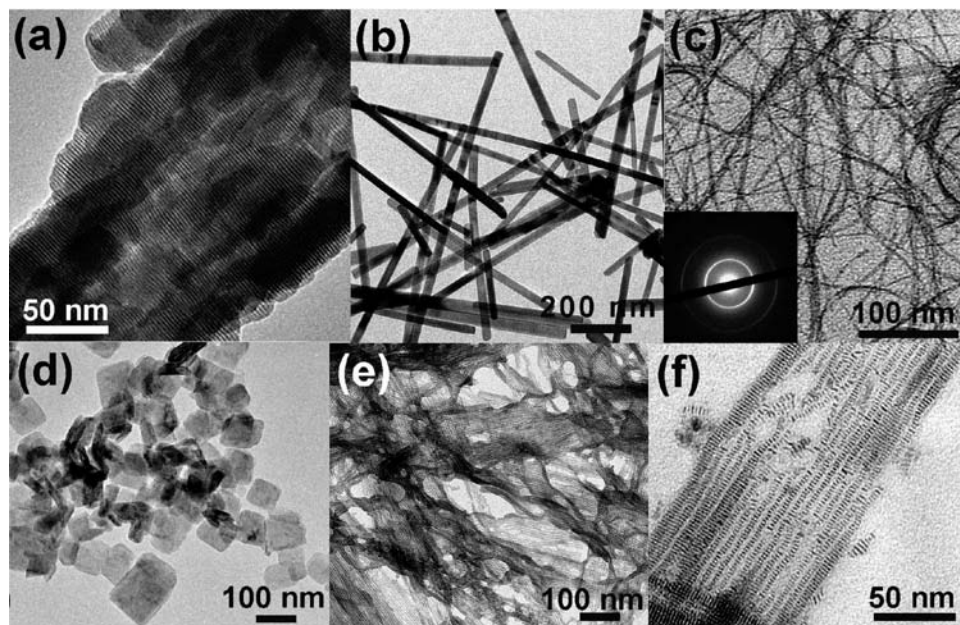


FIGURE 3. (a) TEM image of a neodymium oxide–benzoate nanohybrid. (b) TEM image of lanthanum hydroxide nanofibers. (c) TEM image of tungsten oxide nanowires (inset, SAED pattern). Reproduced from ref 51. Copyright 2006 Wiley-VCH. (d) TEM image of tungstite nanoplatelets synthesized from tungsten chloride in benzyl alcohol. (e and f) TEM images of tungstite nanoplatelets prepared from tungsten chloride in 4-*tert*-butylbenzyl alcohol at different magnifications. Panel 3e reproduced with permission from ref 52. Copyright 2006 The Royal Society of Chemistry.

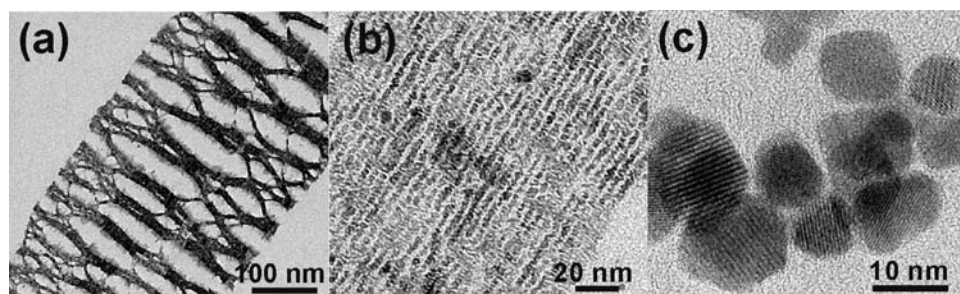


FIGURE 4. TEM images of growing indium tin oxide nanocrystals after (a) 3, (b) 6, and (c) 24 h of reaction time.

alignment on two levels of hierarchy. It is intriguing to see the tremendous effect of 4-*tert*-butylbenzyl alcohol on the crystal growth and assembly of the building blocks in comparison to benzyl alcohol, although these two solvents differ only in the presence of a *tert*-butyl group. Obviously, 4-*tert*-butylbenzyl alcohol fulfills a number of roles that are directly related to its chemical structure. Like benzyl alcohol, the alcohol group provides the oxygen for the formation of tungstite, and its solvation power supports the formation of extended flat nanoplatelets. But in contrast to benzyl alcohol, 4-*tert*-butylbenzyl alcohol with its terminal tertiary butyl group can sterically control both the size of the nanoplatelets and the distance between them.

Another major obstacle on the way to a rational synthesis strategy for inorganic nanoparticles is the fact that the crystallization process of nanoscale materials is still poorly understood. Although crystallization has been studied for decades, it seems that pathways other than just the simple attachment of ions, atoms, or molecules to growing nuclei exist.⁵³ The study of the crystallization of indium tin oxide nanoparticles in benzyl alcohol shed

light on some interesting details and also proved that the organic components were directly involved in the process.⁵⁴ Panels a–c of Figure 4 display TEM images of indium tin oxide nanoparticles after 3, 6, and 24 h of reaction time. It was found that the crystallization process did not proceed along a simple nucleation and growth pathway but involved a two-step process.⁵⁴ First, an intermediary phase was formed, consisting of nanocrystallites that were stabilized by an organic matrix. As a representative example, the sample after 3 h is shown in Figure 4a, with inorganic crystallites of 2–3 nm embedded in an extended, ramified organic network. After 6 h, the sheetlike ribbons seemed to be more compact with larger crystallites (5 nm) and less organics, and the crystallites formed oriented, two-dimensional arrays (Figure 4b). Although the nanoparticles were aligned into superstructures in this organic–inorganic network, they did not exhibit any crystallographic orientation with respect to each other. After 12 h, the intermediate was abruptly transformed into indium tin oxide nanoparticles with the bixbyite structure and with crystallite sizes of 8–12 nm. This step was accompanied by the disappearance of the

organic phase and the loss of the superstructure. The final product after 24 h consisted of disordered agglomerates of nanocrystals of 8–15 nm (Figure 4c).

5. Conclusion

The synthesis of metal oxide nanoparticles in organic solvents, making use of the well-known chemistry of the carbon–oxygen bond, opens the possibility of adapting reaction principles from organic chemistry to the synthesis of inorganic nanomaterials. The thus obtained reaction mechanisms provide answers to the following questions. (i) What is the origin of the oxygen for oxide formation? (ii) How is the oxygen transferred from the source to the metal center? (iii) Which organic species are formed during nanoparticle growth that potentially act as coordinating, size- and shape-controlling ligands? (iv) Which organic species are a result of redox reactions that determine the oxidation state of the metal ions? However, they do not offer any solutions concerning the relationship between a particular synthesis system and the particle morphology. Therefore, the ultimate goal of a rational synthesis strategy, where a sequence of synthesis steps leads to nanoparticles with the desired composition, structure, size, and shape intentionally and in a predicted way, is still not in sight. Although the organic species strongly influence the structural, compositional, and morphological characteristics of the inorganic product and thus offer a versatile tool for tailoring particle size, shape, composition, and surface properties, this is only possible on an empirical basis as long as the organic–inorganic interface is not completely understood on a molecular level and as long as there is no detailed information available about how organic molecules bind and pack on nanocrystal surfaces.⁵⁵

I am thankful to Prof. M. Antonietti for his steady support and enthusiasm. I am also indebted to my current and past group members for their great scientific work. Financial support by the Max Planck Society is acknowledged.

References

- (1) Fierro, J. L. G. *Metal Oxides: Chemistry and Applications*; CRC Press: Boca Raton, FL, 2006.
- (2) Rao, C. N. R.; Raveau, B. *Transition metal oxides*; VCH Publishers Inc.: New York, 1995.
- (3) Cushing, B. L.; Kolesnichenko, V. L.; O'Connor, C. J. Recent advances in the liquid-phase syntheses of inorganic nanoparticles. *Chem. Rev.* **2004**, *104*, 3893–3946.
- (4) Livage, J.; Henry, M.; Sanchez, C. Sol-gel chemistry of transition metal oxides. *Prog. Solid State Chem.* **1988**, *18*, 259–341.
- (5) Hench, L. L.; West, J. K. The sol-gel process. *Chem. Rev.* **1990**, *90*, 33–72.
- (6) Corriu, R. J. P.; Leclercq, D. Recent developments of molecular chemistry for sol-gel processes. *Angew. Chem., Int. Ed.* **1996**, *35*, 1420–1436.
- (7) Niederberger, M.; Garnweitner, G. Organic reaction pathways in the nonaqueous synthesis of metal oxide nanoparticles. *Chem.—Eur. J.* **2006**, *12*, 7282–7302.
- (8) Jun, Y. W.; Choi, J. S.; Cheon, J. Shape control of semiconductor and metal oxide nanocrystals through nonhydrolytic colloidal routes. *Angew. Chem., Int. Ed.* **2006**, *45*, 3414–3439.
- (9) Vioux, A. Nonhydrolytic sol-gel routes to oxides. *Chem. Mater.* **1997**, *9*, 2292–2299.
- (10) Trentler, T. J.; Denler, T. E.; Bertone, J. F.; Agrawal, A.; Colvin, V. L. Synthesis of TiO₂ nanocrystals by nonhydrolytic solution-based reactions. *J. Am. Chem. Soc.* **1999**, *121*, 1613–1614.
- (11) Pinna, N.; Garnweitner, G.; Antonietti, M.; Niederberger, M. Nonaqueous synthesis of high-purity metal oxide nanopowders using an ether elimination process. *Adv. Mater.* **2004**, *16*, 2196–2200.
- (12) Joo, J.; Kwon, S. G.; Yu, J. H.; Hyeon, T. Synthesis of ZnO nanocrystals with cone, hexagonal cone, and rod shapes via nonhydrolytic ester elimination sol-gel reactions. *Adv. Mater.* **2005**, *17*, 1873–1877.
- (13) Li, X.-L.; Peng, Q.; Yi, J.-X.; Wang, X.; Li, Y. Near monodisperse TiO₂ nanoparticles and nanorods. *Chem.—Eur. J.* **2006**, *12*, 2383–2391.
- (14) Narayanaswamy, A.; Xu, H.; Pradhan, N.; Kim, M.; Peng, X. Formation of nearly monodisperse In₂O₃ nanodots and oriented-attached nanoflowers: Hydrolysis and alcoholysis vs pyrolysis. *J. Am. Chem. Soc.* **2006**, *128*, 10310–10319.
- (15) Zhang, Z.; Zhong, X.; Liu, S.; Li, D.; Han, M. Aminolysis route to monodisperse titania nanorods with tunable aspect ratio. *Angew. Chem., Int. Ed.* **2005**, *44*, 3466–3470.
- (16) Goel, S. C.; Chiang, M. Y.; Gibbons, P. C.; Buhro, W. E. New chemistry for the sol-gel process: Acetone as a new condensation reagent. *Mater. Res. Soc. Symp. Proc.* **1992**, *271*, 3–13.
- (17) Steunou, N.; Ribot, F.; Boubekeur, K.; Maquet, J.; Sanchez, C. Ketones as an oxolation source for the synthesis of titanium-oxo-organo clusters. *New J. Chem.* **1999**, *23*, 1079–1086.
- (18) Garnweitner, G.; Antonietti, M.; Niederberger, M. Nonaqueous synthesis of crystalline anatase nanoparticles in simple ketones and aldehydes as oxygen-supplying agents. *Chem. Commun.* **2005**, 397–399.
- (19) Niederberger, M.; Garnweitner, G.; Pinna, N.; Antonietti, M. Nonaqueous and halide-free route to crystalline BaTiO₃, SrTiO₃ and (Ba,Sr)TiO₃ nanoparticles via a formation mechanism involving a C-C bond formation. *J. Am. Chem. Soc.* **2004**, *126*, 9120–9126.
- (20) Murray, C. B.; Norris, D. J.; Bawendi, M. G. Synthesis and characterization of nearly monodisperse CdE (E = S, Se, Te) semiconductor nanocrystallites. *J. Am. Chem. Soc.* **1993**, *115*, 8706–8715.
- (21) de Mello Donegá, C.; Liljeroth, P.; Vanmaekelbergh, D. Physicochemical evaluation of the hot-injection method, a synthesis route for monodisperse nanocrystals. *Small* **2005**, *1*, 1152–1162.
- (22) Kumar, S.; Nann, T. Shape control of II-VI semiconductor nanomaterials. *Small* **2006**, *2*, 316–329.
- (23) Hyeon, T. Chemical synthesis of magnetic nanoparticles. *Chem. Commun.* **2003**, 927–934.
- (24) Park, J.; Lee, E.; Hwang, N.-M.; Kang, M.; Kim, S. C.; Hwang, Y.; Park, J.-G.; Noh, H.-J.; Kim, J.-Y.; Park, J.-H.; Hyeon, T. One-nanometer-scale size-controlled synthesis of monodisperse magnetic iron oxide nanoparticles. *Angew. Chem., Int. Ed.* **2005**, *44*, 2872–2877.
- (25) Song, Q.; Zhang, Z. J. Shape control and associated magnetic properties of spinel cobalt ferrite nanocrystals. *J. Am. Chem. Soc.* **2004**, *126*, 6164–6168.
- (26) Zeng, H.; Rice, P. M.; Wang, S. X.; Sun, S. H. Shape-controlled synthesis and shape-induced texture of MnFe₂O₄ nanoparticles. *J. Am. Chem. Soc.* **2004**, *126*, 11458–11459.
- (27) Zitoun, D.; Pinna, N.; Frolet, N.; Belin, C. Single crystal manganese oxide multipods by oriented attachment. *J. Am. Chem. Soc.* **2005**, *127*, 15034–15035.
- (28) Seo, J.-W.; Jun, Y.-W.; Ko, S. J.; Cheon, J. In situ one-pot synthesis of 1-dimensional transition metal oxide nanocrystals. *J. Phys. Chem. B* **2005**, *109*, 5389–5391.
- (29) Steckel, J. S.; Yen, B. K. H.; Oertel, D. C.; Bawendi, M. G. On the mechanism of lead chalcogenide nanocrystal formation. *J. Am. Chem. Soc.* **2006**, *128*, 13032–13033.
- (30) Liu, H.; Owen, J. S.; Alivisatos, A. P. Mechanistic study of precursor evolution in colloidal group II-VI semiconductor nanocrystal synthesis. *J. Am. Chem. Soc.* **2007**, *129*, 305–312.
- (31) Nel, A.; Xia, T.; Mädler, L.; Li, N. Toxic potential of materials at the nanolevel. *Science* **2006**, *311*, 622–627.
- (32) Garnweitner, G.; Niederberger, M. Overview of nonaqueous and surfactant-free synthesis routes to metal oxide nanoparticles with a strong focus on perovskites. *J. Am. Ceram. Soc.* **2006**, *89*, 1801–1808.
- (33) Niederberger, M.; Garnweitner, G.; Buha, J.; Polleux, J.; Ba, J.; Pinna, N. Nonaqueous synthesis of metal oxide nanoparticles: Review and indium oxide as case study for the dependence of particle morphology on precursors and solvents. *J. Sol-Gel Sci. Technol.* **2006**, *40*, 259–266.
- (34) Niederberger, M.; Bartl, M. H.; Stucky, G. D. Benzyl alcohol and transition metal chlorides as a versatile reaction system for the nonaqueous and low-temperature synthesis of crystalline nano-objects with controlled dimensionality. *J. Am. Chem. Soc.* **2002**, *124*, 13642–13643.

- (35) Ba, J.; Polleux, J.; Antonietti, M.; Niederberger, M. Nonaqueous synthesis of tin oxide nanocrystals and their assembly into ordered porous mesostructures. *Adv. Mater.* **2005**, *17*, 2509–2512.
- (36) Niederberger, M.; Garnweitner, G.; Krumeich, F.; Nesper, R.; Cölfen, H.; Antonietti, M. Tailoring the surface and solubility properties of nanocrystalline titania by a nonaqueous in situ functionalization process. *Chem. Mater.* **2004**, *16*, 1202–1208.
- (37) Polleux, J.; Pinna, N.; Antonietti, M.; Niederberger, M. Growth and assembly of crystalline tungsten oxide nanostructures assisted by bioligation. *J. Am. Chem. Soc.* **2005**, *127*, 15595–15601.
- (38) Polleux, J.; Pinna, N.; Antonietti, M.; Niederberger, M. Ligand-directed assembly of preformed titania nanocrystals into highly anisotropic nanostructures. *Adv. Mater.* **2004**, *16*, 436–439.
- (39) Polleux, J.; Pinna, N.; Antonietti, M.; Hess, C.; Wild, U.; Schlögl, R.; Niederberger, M. Ligand functionality as a versatile tool to control the assembly behavior of preformed titania nanocrystals. *Chem.—Eur. J.* **2005**, *11*, 3541–3551.
- (40) Inoue, M. Glycothermal synthesis of metal oxides. *J. Phys.: Condens. Matter* **2004**, *16*, S1291–S1303.
- (41) Niederberger, M.; Pinna, N.; Polleux, J.; Antonietti, M. A general soft chemistry route to perovskites and related materials: Synthesis of BaTiO₃, BaZrO₃ and LiNbO₃ nanoparticles. *Angew. Chem., Int. Ed.* **2004**, *43*, 2270–2273.
- (42) Ba, J.; Fattakhova Rohlfing, D.; Feldhoff, A.; Brezesinski, T.; Djerdj, I.; Wark, M.; Niederberger, M. Nonaqueous synthesis of uniform indium tin oxide nanocrystals and their electrical conductivity in dependence of the tin oxide concentration. *Chem. Mater.* **2006**, *18*, 2848–2854.
- (43) Gaskins, B. C.; Lannutti, J. J. Room temperature perovskite production from bimetallic alkoxides by ketone assisted oxo supplementation. *J. Mater. Res.* **1996**, *11*, 1953–1959.
- (44) Garnweitner, G.; Hentschel, J.; Antonietti, M.; Niederberger, M. Nonaqueous synthesis of amorphous powder precursors for nanocrystalline PbTiO₃, Pb(Zr,Ti)O₃ and PbZrO₃. *Chem. Mater.* **2005**, *17*, 4594–4599.
- (45) Inoue, M.; Kominami, H.; Inui, T. Novel synthetic method for the catalytic use of thermally stable zirconia: Thermal decomposition of zirconium alkoxides in organic media. *Appl. Catal., A* **1993**, *97*, L25–L30.
- (46) Kominami, H.; Kato, J.; Takada, Y.; Doushi, Y.; Ohtani, B.; Nishimoto, S.; Inoue, M.; Inui, T.; Kera, Y. Novel synthesis of microcrystalline titanium(IV) oxide having high thermal stability and ultra-high photocatalytic activity: Thermal decomposition of titanium(IV) alkoxide in organic solvents. *Catal. Lett.* **1997**, *46*, 235–240.
- (47) Pinna, N.; Garnweitner, G.; Antonietti, M.; Niederberger, M. A general nonaqueous route to binary metal oxide nanocrystals involving a C-C bond cleavage. *J. Am. Chem. Soc.* **2005**, *127*, 5608–5612.
- (48) Buha, J.; Djerdj, I.; Niederberger, M. Nonaqueous synthesis of nanocrystalline indium and zinc oxide in the oxygen-free solvent acetonitrile. *Cryst. Growth Des.* **2007**, *7*, 113–116.
- (49) Pinna, N.; Garnweitner, G.; Beato, P.; Niederberger, M.; Antonietti, M. Synthesis of yttria-based crystalline and lamellar nanostructures and their formation mechanism. *Small* **2005**, *1*, 112–121.
- (50) Karmaoui, M.; Sá Ferreira, R. A.; Mane, A. T.; Carlos, L. D.; Pinna, N. Lanthanide-based lamellar nanohybrids: Synthesis, structural characterization, and optical properties. *Chem. Mater.* **2006**, *18*, 4493–4499.
- (51) Polleux, J.; Gurlo, A.; Barsan, N.; Weimar, U.; Antonietti, M.; Niederberger, M. Template-free synthesis and assembly of single-crystalline tungsten oxide nanowires and their gas-sensing properties. *Angew. Chem., Int. Ed.* **2006**, *45*, 261–265.
- (52) Polleux, J.; Antonietti, M.; Niederberger, M. Ligand and solvent effects in the nonaqueous synthesis of highly ordered anisotropic tungsten oxide nanostructures. *J. Mater. Chem.* **2006**, *16*, 3969–3975.
- (53) Niederberger, M.; Cölfen, H. Oriented attachment and mesocrystals: Non-classical crystallization mechanisms based on nanoparticle assembly. *Phys. Chem. Chem. Phys.* **2006**, *8*, 3271–3287.
- (54) Ba, J.; Feldhoff, A.; Fattakhova Rohlfing, D.; Wark, M.; Antonietti, M.; Niederberger, M. Crystallization of indium tin oxide nanoparticles: From cooperative behavior to individuality. *Small* **2007**, *3*, 310–317.
- (55) Yin, Y.; Alivisatos, A. P. Colloidal nanocrystal synthesis and the organic-inorganic interface. *Nature* **2005**, *437*, 664–670.

AR600035E